

Yangyu Guo and Moran Wang\*

# Thermodynamics of micro- and nano-scale flow and heat transfer: a mini-review

<https://doi.org/10.1515/jnet-2023-0060>

Received July 26, 2023; accepted January 8, 2024; published online January 22, 2024

**Abstract:** The modeling and understanding of micro- and nano-scale transport processes have raised increasing attention and extensive investigation during the past decades. In this mini-review, we aim to summarize our recent progress on the non-equilibrium thermodynamics of micro- and nano-scale flow and heat transfer. Special emphasis is put on the entropy generation at the interface, which plays a dominant role at small scale due to the strong non-equilibrium nature of particle-boundary interaction. We also prove the thermodynamic compatibility of both the macroscopic hydrodynamic equation and the non-equilibrium boundary conditions from the perspective of bulk and interfacial entropy generations respectively, as supported by the kinetic theory of microscopic particles. The present review will contribute to a clearer elaboration of thermodynamics at micro/nano-scale and its statistical mechanical demonstration, and thus will promote its further development in the future.

**Keywords:** non-equilibrium thermodynamics; micro- and nano-scale flow; entropy generation; interfacial transport

## 1 Introduction

With the rapid development of nanoscience and nanotechnology since the end of last century, the modeling and understanding of micro- and nano-scale transport (fluid flow, ion transport, heat transport, etc.) becomes an increasingly important task. The micro- and nano-scale fluid flow has important applications in the MEMS & NEMS (micro/nano-electromechanical system) [1], [2], whereas the ion transport in micro- and nano-channels is relevant to microfluidics and nanofluidics [3], many energy systems and devices (such as supercapacitors [4] and fuel cells [5]). The extensive study on micro- and nano-scale heat conduction in semiconductors and dielectrics has been mainly motivated by the thermal management of micro- and nano-electronics [6], [7], nanostructured thermoelectrics [8], and also advanced machining process [9].

When coming to micro- and nano-scale, the classical macroscopic transport theory based on the continuum assumption may be no long valid. As is known, the Navier–Stokes (N–S) fluid mechanic equation is not capable of describing well gas flows in micro- and nano-channels [2]. The violation of classical Fourier’s law has been shown in heat conduction through nanomaterials by both experiments [10], [11] and modeling [12], [13]. The failure of classical continuum theory has led to the development of generalized macroscopic transport theory for micro- and nano-scale gas flow and heat transfer. The N–S equation was supplemented with slip boundary conditions to model the microscale gas flow in slip regime [2], whereas higher-order moment equations [14] and regularized moment model [15] were proposed to describe the nanoscale gas flow in transition regime. As for the nanoscale non-Fourier heat conduction, there have been a few macroscopic transport models [16], among

---

\*Corresponding author: Moran Wang, Department of Engineering Mechanics and CNMM, Tsinghua University, Beijing 100084, China, E-mail: mrwang@tsinghua.edu.cn

Yangyu Guo, School of Energy Science and Engineering, Harbin Institute of Technology, Harbin 150001, China, E-mail: yyguo@hit.edu.cn

which the phonon hydrodynamic model [17], [18] with natural statistical mechanical (i.e. kinetic theory) basis is one of the most promising candidates.

On the other hand, the classical thermodynamic theory, based on equilibrium or local-equilibrium hypothesis, may also not work well at small scale where strong non-equilibrium effects appear. The classical irreversible thermodynamics (CIT), developed by Onsager [19] and Prigogine [20], was proved to be admissible by the linear and local transport laws of mass, heat and momentum. However, non-linear and non-local effects [15], [21], [22] are significant in nanoscale gas flow and heat transport. As a result, the entropy increase principle (i.e. second law of thermodynamics) based on CIT was shown to fail in non-Fourier heat conduction [23]. Such a defect has been removed by extended thermodynamic theories, represented by rational extended thermodynamics (RET) [24] and extended irreversible thermodynamics (EIT) [25]. In RET and EIT, higher-order dissipative variables (heat flux, stress tensor, etc.) were elevated in the state space to capture the strong non-equilibrium effect at micro- and nano-scale. In this way, the Grad's 13-moment and regularized moment equations for nanoscale gas flow were shown to be compatible with the second law in the frame of EIT [25], [26]. The phonon hydrodynamic model has been also derived from EIT in a phenomenological way [27], [28].

In this mini-review, we aim to summarize our recent work on the thermodynamics of micro- and nano-scale fluid flow and heat transport. This review will include the following three aspects. Firstly, in Section 2, we will discuss the way of statistical thermodynamic average in the analysis of nanoscale fluid flow via atomistic modeling, where a scale gap exists. The validity of the continuum transport theory will be also examined by comparing to the atomistic modeling results. Then in Section 3, we will present our viewpoint on the non-equilibrium thermodynamics of microscale gas flow and heat transfer. The entropy generation at interface, as usually neglected, was derived from kinetic theory of gas and demonstrated to be important at small scale. In Section 4, we will introduce our recent progress on the non-equilibrium thermodynamics for phonon hydrodynamics of nanoscale phonon heat conduction. The emphasis will be put on the previously missing kinetic theoretical derivation for the thermodynamic compatibility of phonon hydrodynamic model. Finally, we will provide a brief summary and some perspectives in Section 5.

## 2 Thermodynamics for transport analysis with scale gap

The molecular dynamics (MD) simulation has been widely used in modeling fluid and ion transport in nanochannels. There is a scale gap since one has to do statistical average of the atomic attributes to obtain the macroscopic variables (density, velocity, pressure, etc.) for transport analysis. In the viewpoint of thermodynamics, those macroscopic variables are meaningful only when the bin size for sampling is sufficiently large, i.e. no smaller than the molecular size.

As an example, we consider the MD simulation of electroosmotic flow in a nanochannel [29]. Very large fluctuations of mass density distribution are observed near the wall of the nanochannel when a very fine bin size of one tenth the molecular diameter is adopted, as shown in Figure 1(a). The largest mass density is even around four times the normal density. However, when we use a bin size of one molecular diameter, the fluctuations are smoothed and an almost uniform density distribution is obtained, as consistent with the continuum theory. The large oscillation of mass density at small bin size is from the inherent microscopic fluctuations of the molecular dynamics. Enough particles in a system are required to do statistical thermodynamic average when we define and calculate macroscopic variables from atomistic simulations. Such an issue is further examined by studying the ion density distribution across the nanochannel, as shown in Figure 1(b). Again, very large fluctuations emerge near the walls when using very fine bin size, and a smooth decaying ion density profile is obtained with a bin size of one molecular diameter. In addition, the MD results are shown to deviate far from the continuum Poisson-Boltzmann (PB) theory in the whole channel, while agree well with that in the diffusion layer. It indicates that the PB theory fails to predict accurately the ion distribution across the whole nanochannel when the thickness of Stern layer near the wall is comparable to or even larger than that of the diffusion layer.

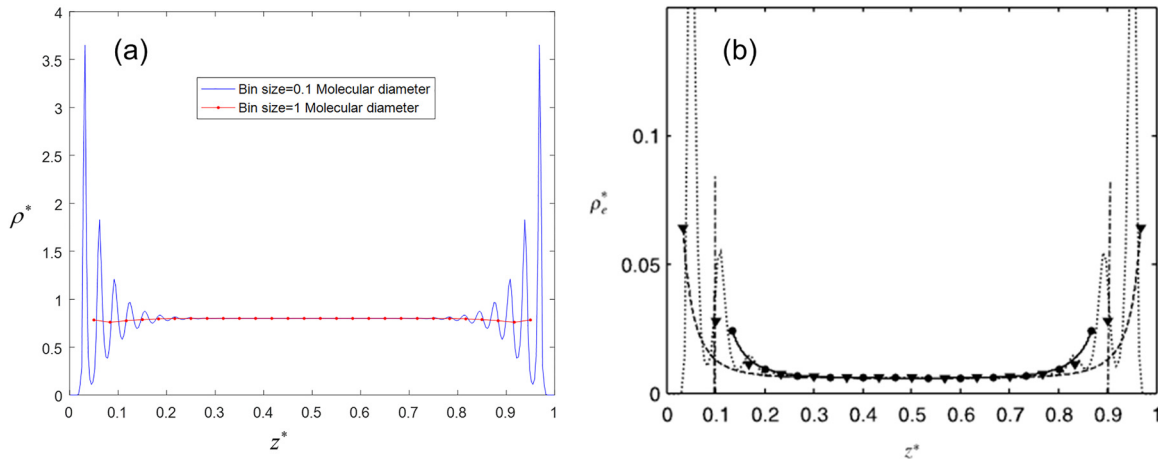


**Figure 1:** Dimensionless mass density and ion density of electroosmotic flow in nanochannel: (a) mass density by MD sampled with 0.1 and 1 molecular diameter bin size respectively; (b) ion density, the dotted line is MD results sampled with finest bin size, the circles and triangles are MD results sampled with one molecular diameter bin size, the triangles are sampled in the whole channel whereas the circles are sampled only in the diffusion layer, the dashed line and solid line are calculated based on Poisson-Boltzmann equation in the whole channel and in the diffusion layer respectively. Figure (b) is reprinted from Ref. [29] with permission.

Indeed, the continuum theory may breakdown when the channel size is too small to validate a proper macroscopic description. A systematic clarification has been recently conducted of the critical size via MD simulation of single-phase liquid flow in nanochannel [30]. The N–S equation with no-slip boundary condition at the wall is valid as long as the channel height is larger than around 100 molecular mean spacings, as demonstrated in Figure 2(a). After considering the solid-like sticky layer near the wall and effective dynamic viscosity of the liquid, the N–S equation remains still valid down to a channel height of 10 molecular mean spacings, as shown in Figure 2(b). When the channel height is even smaller as in the case of  $Nh = 3$  in Figure 2(a), the velocity profile is no longer parabolic. Hydrodynamic model beyond N–S equation or direct atomistic modeling is necessary for this strong non-equilibrium fluid transport.

### 3 Non-equilibrium thermodynamics for microscale gas flow and heat transfer

One of the milestones in non-equilibrium thermodynamics is the optimization of heat and fluid transport processes via the entropy generation minimization principle [31], [32], or second-law analysis [33]. The second-law analysis, originated from CIT, has been extended to microscale gas flow and heat transfer processes [34]–[38]. These works follow the traditional methodology, i.e. computing the entropy generation based on the formula from CIT after solving the temperature and velocity fields. The size effect at microscale is considered by solving the Navier–Stokes–Fourier (N–S–F) equations with velocity slip and temperature jump boundary conditions. A common conclusion was made that the total entropy generation decreased with the increasing  $Kn$  (Knudsen number, defined as the ratio of gas mean free path to channel width) [34], [35]. In our recent study [39], we have shown that the total entropy generation in microscale gas flow and heat transfer should include both the bulk part counted previously [34], [35], and the often neglected interfacial part. As the surface-to-volume ratio increases when the system size is reduced, the interfacial entropy generation plays an increasingly important role and could even change the common trend of the total one. In this section, first we briefly introduce the formula of bulk entropy generation from CIT in Section 3.1. In Section 3.2, we summarize the derivation of interfacial entropy generation from kinetic theory, and verify its non-negativeness as required by the second law. Finally,

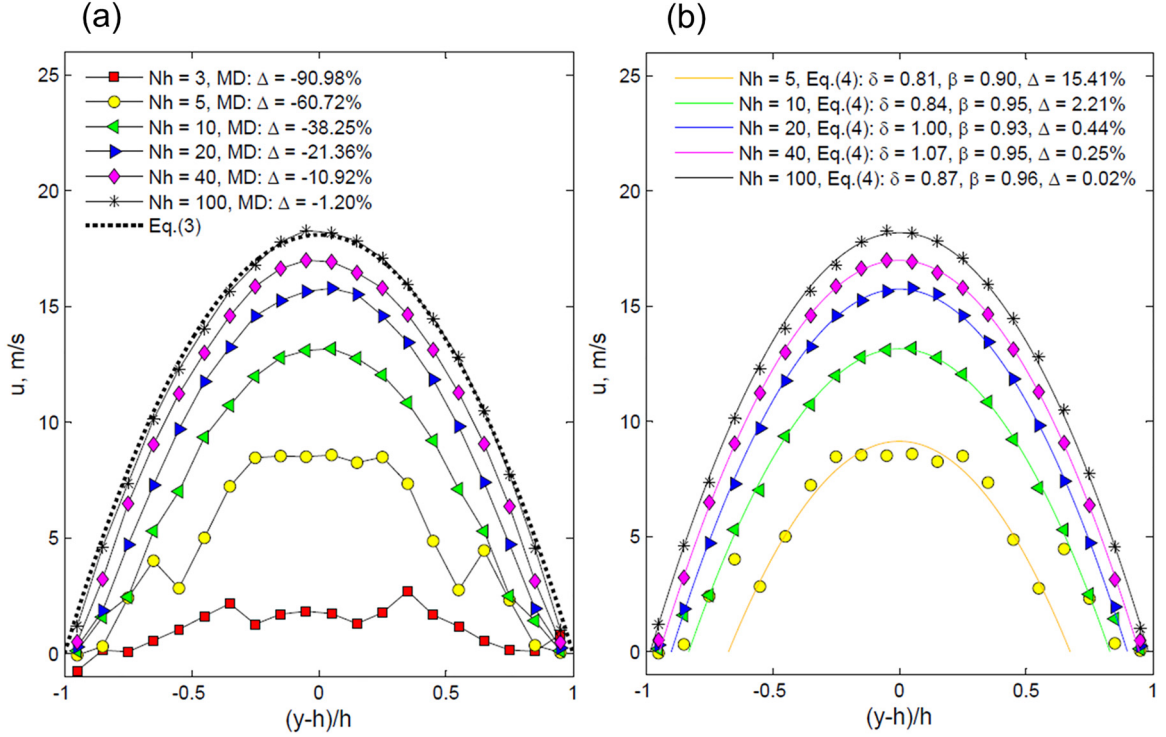


**Figure 2:** Velocity profiles of liquid argon flow in solid argon nanochannel with different dimensionless heights: (a) comparison of MD results to Navier–Stokes equation with non-slip boundary condition at the wall (Eq. (3) in Ref. [30]); (b) comparison of MD results to Navier–Stokes equation with effective viscosity and modified no-slip boundary condition considering the sticky layer near the wall (Eq. (4) in Ref. [30]).  $Nh = 2h/d$ , with  $2h$  the channel height and  $d$  the molecular mean spacing perpendicular to the transport direction.  $\delta d$  is the thickness of sticky layer,  $\beta\mu$  is the effective dynamic viscosity, and  $\Delta$  denotes the relative difference of volume flow rates between MD and continuum theory. Figures are reprinted from Ref. [30] with permission.

in Section 3.3, we demonstrate the comparison of the bulk and interfacial entropy generations in a microscale heat convection.

### 3.1 Bulk entropy generation from CIT

In this work, we consider microscale gas flow in the slip regime, which could be modeled by the N–S–F equations with velocity slip and temperature jump boundary conditions. In the bulk region, the balance equation of entropy (s) is [40]:

$$\rho \frac{ds}{dt} = -\nabla \cdot \mathbf{J}^s + \sigma_b^s, \quad (1)$$

where  $\rho$  denotes the mass density, and the expressions of entropy flux ( $\mathbf{J}^s$ ) and entropy generation ( $\sigma_b^s$ ) are from CIT respectively [40]:

$$\mathbf{J}^s = \frac{\mathbf{q}}{T}, \quad (2)$$

$$\sigma_b^s = \frac{\lambda}{T^2} (\nabla T)^2 + \frac{\mu}{T} \left[ \nabla \mathbf{u} + (\nabla \mathbf{u})^T \right] : \nabla \mathbf{u} - \frac{2}{3} \frac{\mu}{T} (\nabla \cdot \mathbf{u})^2, \quad (3)$$

where  $\mathbf{q}$ ,  $T$ , and  $\mathbf{u}$  represent respectively the heat flux, temperature and velocity,  $\lambda$  and  $\mu$  denote the thermal conductivity and dynamic viscosity of the fluid respectively, and the superscript ‘T’ denotes the transpose of a second-order tensor. For incompressible fluid flow ( $\nabla \cdot \mathbf{u} = 0$ ) considered in this work, the bulk entropy generation in Eq. (3) is reduced to:

$$\sigma_b^s = \frac{\lambda}{T^2} (\nabla T)^2 + \frac{\mu}{T} \left[ \nabla \mathbf{u} + (\nabla \mathbf{u})^T \right] : \nabla \mathbf{u}. \quad (4)$$

### 3.2 Derivation of interfacial entropy generation from kinetic theory

The velocity slip and temperature jump at the boundaries in microscale gas flow come from the non-equilibrium interaction between the gas and wall. Here we provide the idea of deriving the interfacial entropy generation from kinetic theory of gases [39]. For simplicity, we assume negligible coupling between fluid flow and heat transport, and evaluate the entropy generation at the interface induced by velocity slip and temperature jump separately, as shown in Figure 3(a) and (b).

The starting point is the fundamental Boltzmann transport equation (BTE) under BGK relaxation approximation [41], [42]:

$$\frac{\partial f}{\partial t} + \mathbf{c} \cdot \frac{\partial f}{\partial \mathbf{x}} = -\frac{f - f_{\text{eq}}}{\tau}, \quad (5)$$

where  $f = f(\mathbf{x}, \mathbf{c}, t)$  is the velocity distribution function dependent on space ( $\mathbf{x}$ ) and time ( $t$ ),  $\mathbf{c}$  being the molecular velocity,  $\tau$  is the relaxation time, and the equilibrium distribution function  $f_{\text{eq}}$  is the local Maxwell-Boltzmann distribution:

$$f_{\text{eq}} = \frac{\rho}{m} \left( \frac{m}{2\pi k_B T} \right)^{3/2} \exp \left[ -\frac{m(c_\alpha - u_\alpha)^2}{2k_B T} \right], \quad (6)$$

where  $m$  is the molecular mass, with  $k_B$  the Boltzmann constant. The Einstein's rule of summation is adopted hereafter, with the subscripts  $\alpha$  ( $\beta, \dots$ ) the indices of Cartesian coordinate components. Since the fluid flow in bulk region is described by the N-S-F equations, the first-order Chapman-Enskog expansion solution of Eq. (5) is adopted for further analysis [41], [43]:

$$f = f_{\text{eq}} - \left[ \begin{aligned} & \frac{m^2 f_{\text{eq}}}{\rho(k_B T)^2} (c_\alpha - u_\alpha)(c_\beta - u_\beta) \mu \frac{\partial u_\alpha}{\partial x_\beta} - \frac{m^2 f_{\text{eq}}}{3\rho(k_B T)^2} (c_\alpha - u_\alpha)(c_\alpha - u_\alpha) \mu \frac{\partial u_\beta}{\partial x_\beta} \\ & - \frac{m^2 f_{\text{eq}}}{\rho(k_B T)^2} (c_\alpha - u_\alpha) \lambda \frac{\partial T}{\partial x_\alpha} + \frac{m^3 f_{\text{eq}}}{5\rho(k_B T)^3} (c_\alpha - u_\alpha)(c_\alpha - u_\alpha)(c_\beta - u_\beta) \lambda \frac{\partial T}{\partial x_\beta} \end{aligned} \right]. \quad (7)$$

By multiplying  $-k_B \ln f$  on both sides of the BTE in Eq. (5) and integrating over the molecular velocity space, we obtain the entropy balance equation in Eq. (1), together with the kinetic definitions of entropy density and entropy flux respectively [25]:

$$\rho s = -k_B \int f \ln f d\mathbf{c}, \quad (8)$$

$$\mathbf{J}^s = -k_B \int (\mathbf{c} - \mathbf{u}) f \ln f d\mathbf{c}. \quad (9)$$

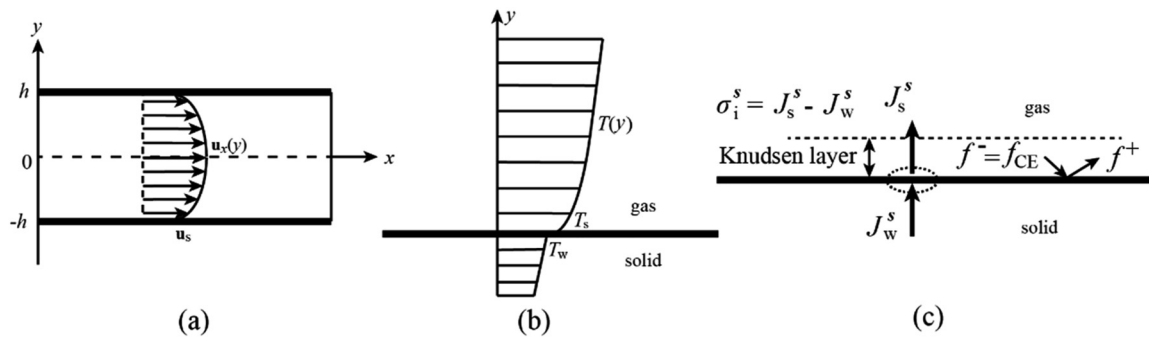


**Figure 3:** Derivation of interfacial entropy generation in microscale gas flow and heat transport: (a) isothermal microscale gas flow with velocity slip, (b) microscale gas conduction with temperature jump, (c) kinetic theory foundation of interfacial entropy generation. Figures are reproduced from Ref. [39].

Let's first derive the interfacial entropy generation induced by velocity slip as shown in Figure 3(a). In this case, from Eq. (7), the non-equilibrium distribution function of gases incident onto the wall from the bulk region is reduced to:

$$f^- = f_{\text{eq}}^- \left[ 1 - \frac{m^2}{\rho(k_B T)^2} (c_x - u_s) c_y \mu \left( \frac{\partial u_x}{\partial y} \right)_s \right], \quad (10)$$

where the subscript 's' denotes the variable of gas at the wall surface,  $u_s$  is the gas slip speed at the wall, and the local equilibrium distribution function is:

$$f_{\text{eq}}^- = \frac{\rho}{m} \left( \frac{m}{2\pi k_B T} \right)^{3/2} \exp \left[ -\frac{(c_x - u_s)^2 + c_y^2 + c_z^2}{2k_B T/m} \right]. \quad (11)$$

The basic idea of deriving the interfacial entropy generation is computing it as the difference of entropy flux of gas and entropy flux of solid side at the wall interface, as illustrated in Figure 3(c) [39]:

$$\sigma_i^s = J_s^s - J_w^s = J_s^s = -k_B \int c_y f_s \ln f_s dc. \quad (12)$$

The entropy flux of solid side  $J_w^s = 0$  since we consider isothermal fluid flow in this case. In Eq. (12), the velocity distribution of gases at the wall is:

$$f_s = \begin{cases} f^-, & \text{for } c_y < 0 \\ f^+, & \text{for } c_y > 0 \end{cases}, \quad (13)$$

where the distribution function of gases reflected from the wall  $f^+$  is related to  $f^-$  through the gas-surface interaction model. For simplicity, the fully diffuse Maxwell model is considered here:  $f^+ = f_0(T_w)$ , with  $f_0$  the global Maxwell–Boltzmann distribution. Putting Eq. (13) into Eq. (12) and integrating over the molecular velocity space, we obtain the explicit expression of interfacial entropy generation for velocity slip [39]:

$$\sigma_i^s = \frac{\mu}{\pi T} \Lambda \left[ \left( \frac{\partial u_x}{\partial y} \right)_s \right]^2. \quad (14)$$

In Eq. (14), the gas mean free path  $\Lambda$  has been related to the dynamic viscosity  $\mu$  as [41]:  $\mu = \frac{1}{2} \rho \bar{c} \Lambda = \rho \Lambda \sqrt{2k_B T / \pi m}$ . With the gas slip speed in the fully diffuse Maxwell model:  $u_s = \Lambda \left( \frac{\partial u_x}{\partial y} \right)_s$ , Eq. (14) is slightly reformulated into:

$$\sigma_i^s = \frac{\mu}{\pi T} u_s \left( \frac{\partial u_x}{\partial y} \right)_s. \quad (15)$$

Let's then consider the derivation of interfacial entropy generation induced by temperature jump, as shown in Figure 3(b). In principle, it could be derived through a similar procedure to that of velocity slip. However, it is a non-trivial task to obtain the entropy flux of non-equilibrium solid side at the interface because of the distinction between kinetic theories of solids and gases. Thus we simply estimate the entropy generation at the interface as the difference of entropy fluxes at the gas side and at the solid side assuming the classical form in Eq. (2) [39]:

$$\sigma_i^s = J_w^s - J_s^s = \frac{q_n}{T_w} - \frac{q_n}{T_s}. \quad (16)$$

A further investigation of the microscopic foundation of the gas-solid interfacial entropy generation is pending in a future study.

To sum up, the interfacial entropy generations in Eq. (15) and (16) are proportional to the slip speed and temperature jump at the wall. The interfacial entropy generation of velocity slip is obviously non-negative, as seen in Eq. (14). Also, the interfacial entropy generation of temperature jump is non-negative, since  $T_w < T_s$ . Therefore, the expressions of entropy generation at the interface are well compatible with the second law of

thermodynamics. The non-equilibrium thermodynamics for microscale gas flow and heat transfer are summarized in Table 1. In the limit of macroscopic scale, the interfacial entropy generation is vanishingly small due to the negligible velocity slip and temperature jump. However, it becomes an appreciable contribution at microscale, where those non-equilibrium slip and jump phenomena are salient. A quantitative demonstration will be given in the following sub-section.

### 3.3 Bulk versus interfacial entropy generation at microscale

In this sub-section, we aim to quantify the entropy generation in microscale heat convection through a micro-pipe with a radius  $R$ , as shown in Figure 4(a). The hydrodynamically and thermally fully-developed steady-state

**Table 1:** Summary of non-equilibrium thermodynamics for microscale gas flow and heat transport.

Non-equilibrium phenomena	Transport or constitutive equations	Entropy generation
Fluid flow & heat conduction	Navier–Stokes–Fourier equations	$\sigma_b^s = \frac{\lambda}{T^2} (\nabla T)^2 + \frac{\mu}{T} [\nabla \mathbf{u} + (\nabla \mathbf{u})^T] : \nabla \mathbf{u} \geq 0$
Velocity slip	$u_s = \Lambda \left( \frac{\partial u_x}{\partial y} \right)_s$	$\sigma_i^s = \frac{\mu}{\pi T} u_s \left( \frac{\partial u_x}{\partial y} \right)_s = \frac{\mu}{\pi \Lambda T} u_s^2 \geq 0$
Temperature jump	$q_n = G(T_s - T_w)$	$\sigma_i^s = \frac{q_n}{T_w} - \frac{q_n}{T_s} = \frac{q_n^2}{GT_w T_s} \geq 0$

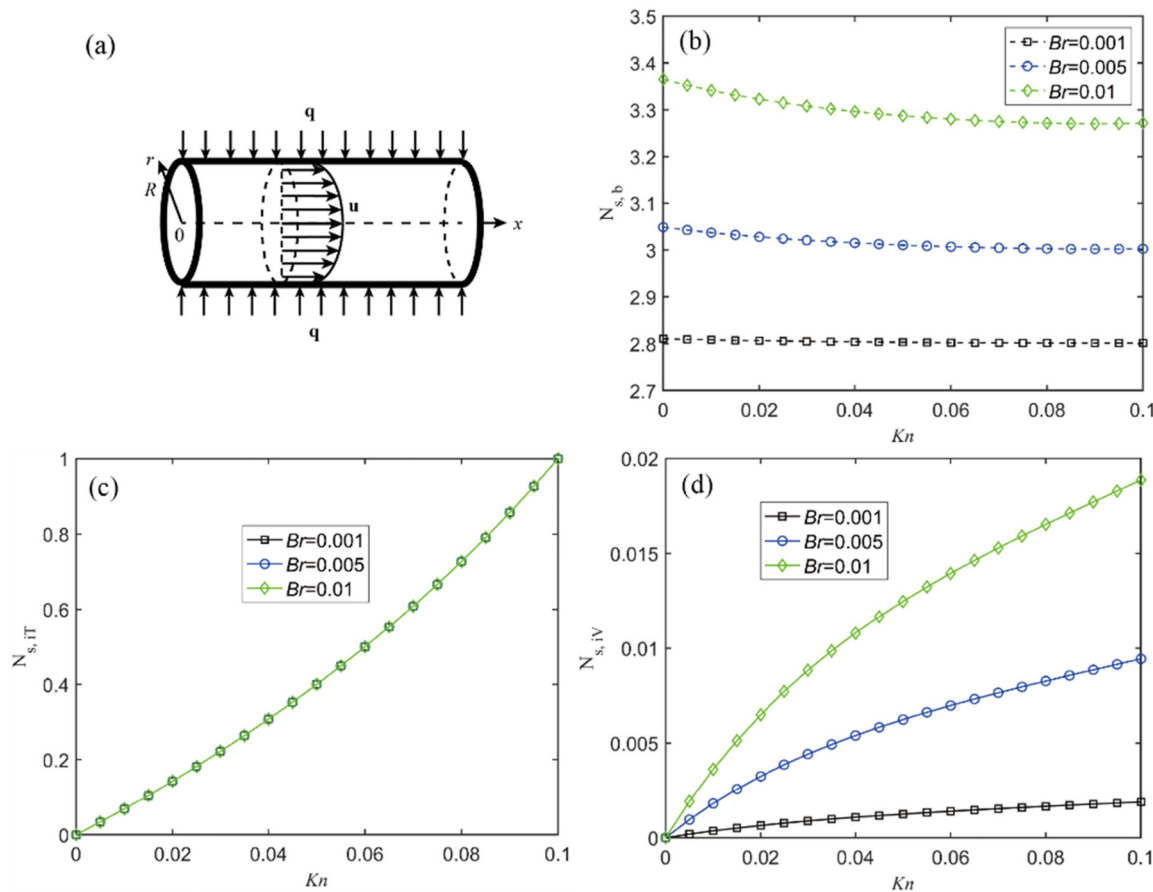


**Figure 4:** Thermodynamic analysis of fully-developed microscale gas heat convection: (a) schematic of the physical model; (b) bulk entropy generation number; (c) interfacial entropy generation number induced by temperature jump; (d) interfacial entropy generation number induced by velocity slip. Three different Brinkman numbers are considered:  $Br = 0.001, 0.005, 0.01$ . Figures are reproduced from Ref. [39].

laminar gas flow is studied, with the axial heat conduction neglected and constant fluid properties considered [39], [44]. The velocity and temperature fields are computed by an analytical solution of N–S–F equation with first-order velocity slip and temperature jump boundary conditions, with the details given in Ref. [39]. Then the entropy generation can be calculated based on Eq. (4), (15) and (16). The source of entropy generation includes four parts: (i) viscous fluid flow, and (ii) heat conduction in the bulk region; (iii) velocity slip, and (iv) temperature jump at the wall. Thus the total entropy generation is expressed as:

$$S_{\text{gen}} = S_{\text{gen,H}} + S_{\text{gen,F}} + S_{\text{gen,V}} + S_{\text{gen,T}}, \quad (17)$$

where the subscripts ‘H’, ‘F’, ‘V’ and ‘T’ denote ‘heat conduction’, ‘fluid flow’, ‘velocity slip’ and ‘temperature jump’ respectively. Taking a volume element  $dV = A_c dx$  along the axial direction of the pipe within  $(x, x + dx)$ , with  $A_c$  the cross-sectional area, we compute each part of the entropy generation as follows [39]:

$$S_{\text{gen,H}} = \int_V \sigma_H^s dV = \int_V \frac{\lambda}{T^2} (\nabla T)^2 dV = dx \int_{A_c} \frac{\lambda}{T^2} \left( \frac{\partial T}{\partial r} \right)^2 dA, \quad (18)$$

$$S_{\text{gen,F}} = \int_V \sigma_F^s dV = \int_V \frac{\mu}{T} \left( \frac{du}{dr} \right)^2 dV = dx \int_{A_c} \frac{\mu}{T} \left( \frac{du}{dr} \right)^2 dA, \quad (19)$$

$$S_{\text{gen,V}} = \int_{\Sigma} \sigma_V^s d\Sigma = \int_{\Sigma} \frac{\mu}{\pi T_s} u_s \left( \frac{du}{dr} \right)_s d\Sigma = P dx \frac{\mu}{\pi T_s} u_s \left( \frac{du}{dr} \right)_s, \quad (20)$$

$$S_{\text{gen,T}} = \int_{\Sigma} \sigma_T^s d\Sigma = \int_{\Sigma} q \left( \frac{1}{T_s} - \frac{1}{T_w} \right) d\Sigma = P dx q \left( \frac{1}{T_s} - \frac{1}{T_w} \right). \quad (21)$$

In Eqs. (20) and (21),  $\Sigma = P dx$  is the surface element of the volume element, with  $P$  the perimeter of the circular cross-section of the micro-pipe. For convenience, a dimensionless entropy generation number is introduced as:

$$N_s = \frac{S_{\text{gen}}}{\frac{\lambda}{R^2} A_c dx} = \frac{S_{\text{gen}}}{\pi \lambda dx}. \quad (22)$$

Our definition of entropy generation number in Eq. (22) follows a previous study [35], where  $\lambda/R^2 A_c dx$  denotes a reference entropy generation inside the volume element  $dV$ .

The entropy generation numbers of viscous flow and heat conduction in the bulk region, and of temperature jump and velocity slip are shown in Figure 4(b)–(d) respectively. Three different Brinkman numbers ( $Br$ , defined as the ratio of viscous dissipation heat to external heat supply:  $Br = \mu u_m^2 / 2Rq$ ) are considered. Generally, the bulk entropy generation number in Figure 4(b) decreases with increasing  $Kn$  (defined as  $Kn = \Lambda / 2R$ ), which could be explained by the more flattened profiles and smaller gradients of velocity and temperature fields due to larger velocity slip and temperature jump at the wall. In contrast, the interfacial entropy generation number in Figure 4(c) and (d) increases with increasing  $Kn$ , as both the non-equilibrium slip and jump are correspondingly enhanced. As a result, the total entropy generation number, including the contribution from both the bulk region and interfacial region, will increase as  $Kn$  increases, as shown in Figure 5. This is a reverse trend compared to that in previous works [34]–[38] considering only the irreversibility from heat and fluid transport in the bulk region. The interfacial irreversibility becomes increasingly important at small scale, where the equilibration and thermalization between the gas molecules and solid wall is more difficult, i.e. a stronger non-equilibrium effect emerges.

## 4 Non-equilibrium thermodynamics for phonon hydrodynamics of micro- and nano-scale heat transport

Owing to the failure of classical Fourier’s law and expensive cost of directly solving phonon BTE for micro- and nano-scale heat conduction, people have been trying to seek macroscopic transport models with simpler

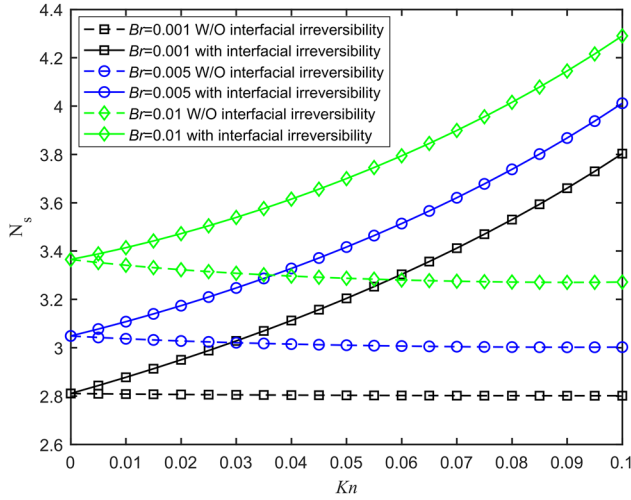


**Figure 5:** Total entropy generation number of microscale gas heat convection versus  $Kn$ . The solid lines with symbols represent the results counting both bulk and interfacial entropy generation, whereas the dashed lines with symbols represent the results counting only bulk entropy generation. Three different Brinkman numbers are considered:  $Br = 0.001, 0.005, 0.01$ . The figure is reproduced from Ref. [39].

mathematical description and clearer physical picture [16]. In our recent study [18], we have derived a macroscopic phonon hydrodynamic model from phonon BTE by regularized moment method. The starting point is the phonon BTE under single mode relaxation time (SMRT) approximation:

$$\frac{\partial f}{\partial t} + \mathbf{v}_g \cdot \nabla f = -\frac{f - f_R^{\text{eq}}}{\tau_R}, \quad (23)$$

where  $\mathbf{v}_g$  and  $\tau_R$  are the group velocity and relaxation time of phonons respectively, and the equilibrium distribution  $f_R^{\text{eq}}$  is the Bose–Einstein distribution. The basic idea of the regularized moment method [15], [18] is a perturbative expansion of the phonon distribution function around a four-moment non-equilibrium solution obtained by maximum entropy principle. In this way, the derived macroscopic equation will be able to describe heat transport in a stronger nonequilibrium regime, as given below [18]:

$$\tau_R \frac{\partial \mathbf{q}}{\partial t} + \mathbf{q} = -\lambda \nabla T + \frac{1}{5} \Lambda^2 \left[ \nabla^2 \mathbf{q} + \frac{1}{3} \nabla (\nabla \cdot \mathbf{q}) \right], \quad (24)$$

where  $\Lambda$  is the mean free path of phonons here. Compared to Fourier’s law, Eq. (24) contains relaxation term and non-local terms of heat flux, which are crucial to capture the size effects from both small time and space scales. Equation (24) is known to be the Guyer–Krumhansl type heat conduction equation, which was originally derived for phonon hydrodynamics in crystals at low temperatures [45] and has been also shown to well explain the heat pulse propagation in macro-scale heterogeneous materials at room temperatures in recent years [46]–[48]. The corresponding solution of phonon distribution function to Eq. (23) is written as [18]:

$$f = f_R^{\text{eq}} + \frac{3}{C_V v_g^2} \frac{\partial f_R^{\text{eq}}}{\partial T} q_\alpha v_{g\alpha} + \frac{\tau_R}{C_V} \frac{\partial q_\alpha}{\partial x_\alpha} \frac{\partial f_R^{\text{eq}}}{\partial T} - \frac{3\tau_R}{C_V v_g^2} v_{g\alpha} v_{g\beta} \frac{\partial q_\alpha}{\partial x_\beta} \frac{\partial f_R^{\text{eq}}}{\partial T}, \quad (25)$$

where  $C_V$  denotes the volumetric heat capacity of the solid.

In the following, we will demonstrate that the phonon hydrodynamic equation (24) is compatible with second law of thermodynamics. In Section 4.1, the entropy density and flux will be derived from the phonon kinetic theory, and the entropy generation will be proved to be positive-definite in the frame of EIT. In Section 4.2, we will derive the expression of interfacial entropy generation and show its non-negativeness as required by the second law.

#### 4.1 Entropy density, flux, and generation in the bulk region

Phonons are bosons, and the statistical mechanical definition of entropy density is expressed as [49], [50]:

$$s = -k_B \int [f \ln f - (1 + f) \ln(1 + f)] \, d\mathbf{k}, \quad (26)$$

where  $\mathbf{k}$  denotes the phonon wave vector. The time derivative of entropy density is calculated from Eq. (26) as:

$$\frac{\partial s}{\partial t} = -k_B \int \left\{ \frac{\partial(f \ln f)}{\partial t} - \frac{\partial[(1 + f) \ln(1 + f)]}{\partial t} \right\} \, d\mathbf{k}. \quad (27)$$

With the help of phonon BTE in Eq. (23), Eq. (27) yields the balance equation of entropy similar to Eq. (1) and the kinetic definition of entropy flux:

$$\mathbf{J}^s = -k_B \int \mathbf{v}_g [f \ln f - (1 + f) \ln(1 + f)] \, d\mathbf{k}. \quad (28)$$

Putting the non-equilibrium solution of phonon distribution function in Eq. (25) into the kinetic definition in Eq. (26) and integrating over the wave vector space, we obtain the explicit expression of entropy density as:

$$s = s_{\text{eq}} - \frac{\tau_R}{2\lambda T^2} \mathbf{q} \cdot \mathbf{q} - \frac{\tau_R}{5\lambda T^2} \Lambda^2 (\nabla \mathbf{q})_o^s : (\nabla \mathbf{q})_o^s. \quad (29)$$

In Eq. (29), the equilibrium entropy density is defined as:

$$s_{\text{eq}} = -k_B \int [f_R^{\text{eq}} \ln f_R^{\text{eq}} - (1 + f_R^{\text{eq}}) \ln(1 + f_R^{\text{eq}})] \, d\mathbf{k}. \quad (30)$$

The symmetric traceless part of the gradient of heat flux  $\nabla \mathbf{q}$  is fully expressed as:

$$(\nabla \mathbf{q})_o^s = \frac{1}{2} [\nabla \mathbf{q} + (\nabla \mathbf{q})^T] - \frac{1}{3} (\nabla \cdot \mathbf{q}) \mathbf{I}, \quad (31)$$

with  $\mathbf{I}$  the unit tensor. Similarly, putting Eq. (25) into Eq. (28) and integrating over the wave vector space, we obtain the explicit expression of entropy flux:

$$\mathbf{J}^s = \frac{\mathbf{q}}{T} + \frac{2\Lambda^2}{5\lambda T^2} \mathbf{q} \cdot (\nabla \mathbf{q})_o^s. \quad (32)$$

The details of the derivation of Eq. (29) and (32) can be found in our previous work [50].

With the explicit expressions of phonon entropy density and flux, now we will show that the corresponding phonon hydrodynamic equation (24) is compatible with the second law in the frame of EIT. In EIT, the entropy density is a function of the state variables:  $s = s(e, \mathbf{q}, (\nabla \mathbf{q})_o^s)$ , as inferred from Eq. (29), with  $e$  the energy density. The generalized Gibbs relation is thus obtained [25], [50]:

$$ds = \frac{de}{T} - \frac{\tau_R}{\lambda T^2} \mathbf{q} \cdot d\mathbf{q} - \frac{2\tau_R}{5\lambda T^2} \Lambda^2 (\nabla \mathbf{q})_o^s : d(\nabla \mathbf{q})_o^s. \quad (33)$$

Eq. (33) is slightly rewritten into the time derivative form:

$$\frac{ds}{dt} = \frac{1}{T} \frac{de}{dt} - \frac{\tau_R}{\lambda T^2} \mathbf{q} \cdot \frac{d\mathbf{q}}{dt} - \frac{2\tau_R}{5\lambda T^2} \Lambda^2 (\nabla \mathbf{q})_o^s : \frac{d(\nabla \mathbf{q})_o^s}{dt}. \quad (34)$$

With the help of the balance equations of energy ( $de/dt + \nabla \cdot \mathbf{q} = 0$ ) and entropy, together with the entropy flux in Eq. (32), finally we derive the explicit expression of entropy generation in bulk region as:

$$\sigma_b^s = \frac{\mathbf{q}}{\lambda T^2} \cdot \left\{ -\lambda \nabla T - \tau_R \frac{d\mathbf{q}}{dt} + \frac{\Lambda^2}{5} \left[ \frac{1}{3} \nabla (\nabla \cdot \mathbf{q}) + \nabla^2 \mathbf{q} \right] \right\} + \frac{2\Lambda^2}{5\lambda T^2} (\nabla \mathbf{q})_o^s : (\nabla \mathbf{q})_o^s. \quad (35)$$

With the phonon hydrodynamic equation (24) at hand, the entropy generation in Eq. (35) becomes:

$$\sigma^s = \frac{\mathbf{q} \cdot \mathbf{q}}{\lambda T^2} + \frac{2\Lambda^2}{5\lambda T^2} (\nabla \mathbf{q})_o^s : (\nabla \mathbf{q})_o^s. \quad (36)$$

Equation (36) admits exactly a positive-definite quadratic form, i.e.  $\sigma^s \geq 0$ . In other words, even in micro-scale and nanoscale heat conduction, the macroscopic transport equation of phonons still satisfies the second law in the frame of EIT. Note that the essence of EIT is to postulate the expressions of entropy and entropy flux with forms as in Eq. (29) and (32) and derive a constitutive heat transport equation from the entropy principle (i.e., second law) [25], [51], [52]. However, the phonon kinetic theory is used here to provide a microscopic interpretation of the entropy and entropy flux, as well as the transport coefficients in the phonon hydrodynamic equation (24).

## 4.2 Interfacial entropy generation

In modeling micro- and nano-scale heat conduction, the phonon hydrodynamic equation (24) should be also supplemented with boundary conditions. In our previous work [18], we have derived from phonon kinetic theory the heat flux tangential retardant (HFTR) boundary condition for in-plane heat transport as shown in Figure 6(a):

$$q_{xs} = \frac{8}{15} \Lambda \left( \frac{\partial q_x}{\partial y} \right)_s. \quad (37)$$

The heat flux reduction within the Knudsen layer near the boundary represents the strong non-equilibrium between the phonons inside the transport channel and the boundary. Such non-equilibrium effect will also induce entropy generation at the boundary, similar to the situation in microscale gas flow in Section 3.2. Actually, the thermodynamic consistency of the boundary conditions in nanoscale heat transport has been already investigated by introducing the interfacial entropy generation in a phenomenological way [53], [54]. Here, we will provide a kinetic theoretical derivation of the entropy generation at the lower boundary in in-plane phonon heat transport, as shown in Figure 6(b).

Following the same idea of entropy balance at the interface in Section 3.2, we have the interfacial entropy generation as:

$$\sigma_i^s = -k_B \int v_{gy} [f_s \ln f_s - (1 + f_s) \ln(1 + f_s)] d\mathbf{k}, \quad (38)$$

where the distribution function of phonons at the boundary is:

$$f_s = \begin{cases} f^-, & \mathbf{k} \cdot \mathbf{n} < 0 \\ f^+, & \mathbf{k} \cdot \mathbf{n} > 0 \end{cases}, \quad (39)$$

with  $\mathbf{n}$  the normal unit vector at the boundary, as illustrated in Figure 6(b). The distribution function of incident phonons on the boundary is exactly that in Eq. (25), which is reduced to the following expression in the present in-plane case:

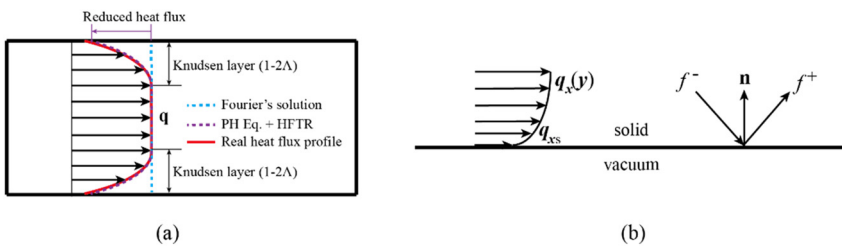


**Figure 6:** Non-equilibrium thermodynamics for micro- and nano-scale phonon heat transport: (a) non-equilibrium effect and phonon hydrodynamic modeling; (b) schematic of in-plane heat transport for derivation of interfacial entropy generation. Figure (a) is reprinted from Ref. [18], whereas Figure (b) is reproduced from Ref. [50].

**Table 2:** Summary of the brief history of non-equilibrium thermodynamics for transport theory together with the kinetic theory support.

Hydrodynamic equation	Kinetic theory method	Thermodynamic theory
Navier–Stokes–Fourier equations	Chapman–Enskog expansion (1916) [41]	Classical irreversible thermodynamics (CIT) (1930s–1940s) [19], [20]
Grad’s 13-moment equations, R13 moment equations	Grad’s moment method (1949) [14], regularization (2003) [15]	Extended thermodynamics (RET, EIT) (1960s–1980s) [24], [25]
Phonon hydrodynamic models	Eigen-state analysis (1966) [45], regularized moment method (2018) [18]	EIT frame (since 1990s) [27]

$$f^- = f_R^{\text{eq}} + \frac{3}{C_V v_g^2} \frac{\partial f_R^{\text{eq}}}{\partial T} q_{xs} v_{gx} - \frac{3\tau_R}{C_V v_g^2} v_{gx} v_{gy} \left( \frac{\partial q_x}{\partial y} \right)_s \frac{\partial f_R^{\text{eq}}}{\partial T}. \quad (40)$$

As consistent with the derivation of the HFTR boundary condition in Eq. (37), the distribution function of reflected phonons is related to that of incident ones via the fully thermalizing diffuse phonon-boundary scattering [55]:

$$f^+ = f_R^{\text{eq}}. \quad (41)$$

Putting Eqs. (39)–(41) into Eq. (38) and conducting integration over the wave vector space, we finally obtain the interfacial entropy generation as [50]:

$$\sigma_i^s = \frac{9}{32} \frac{q_{xs}^2}{C_V v_g T^2} + \frac{3}{32} \frac{\tau_R^2 v_g}{C_V T^2} \left( \frac{\partial q_x}{\partial y} \right)_s^2 + \frac{3}{10} \frac{\tau_R}{C_V T^2} q_{xs} \left( \frac{\partial q_x}{\partial y} \right)_s. \quad (42)$$

With the help of HFTR boundary condition in Eq. (37), Eq. (42) is reformulated into:

$$\sigma_i^s = \frac{801}{2048} \frac{\Lambda q_{xs}^2}{\lambda T^2} \approx 0.4 \frac{\Lambda q_{xs}^2}{\lambda T^2}. \quad (43)$$

The non-negative quadratic form of interfacial entropy generation in Eq. (43) infers that the non-equilibrium boundary condition for the phonon hydrodynamic equation (24) is also compatible with the second law of thermodynamics.

To sum up, the crucial contribution of our work in Section 4 is that we provide a statistical mechanical (i.e. kinetic theory) demonstration for the phenomenological EIT scheme for phonon hydrodynamic model for micro- and nano-scale heat conduction in solids. Thus we contribute to a further step in the understanding of non-equilibrium thermodynamics for heat and fluid transport theory, as summarized in Table 2. Note that we have also included the classical phonon hydrodynamic equation derived for heat transport at low temperatures [45], [56]. In contrast, the phonon hydrodynamic model discussed in this paper is mainly focused on the non-Fourier heat conduction at micro- and nano-scale around ordinary temperatures [18], [57].

## 5 Summary and perspectives

In summary, the present mini-review mainly includes the following points: (i) statistical thermodynamic average should be carefully treated in atomistic modeling and analysis of nanoscale transport processes; (ii) the irreversibility at the interface, as counted by the interfacial entropy generation, plays an important role and may even determine the overall trend of the results in thermodynamic analysis of microscale gas flow and heat transfer; (iii) the macroscopic hydrodynamic model for micro- and nano-scale heat conduction can be derived from the second law in the frame of extended irreversible thermodynamics, with a microscopic support from the kinetic theory of phonons.

As a perspective, the interfacial irreversibility in gas flow and heat transfer at nanoscale, i.e. in transition regime, is pending to investigate. The transport is more non-equilibrium and the interfacial entropy generation

may be dominant, compared to the microscale transport considered in Section 3. In terms of the micro- and nano-scale heat conduction, our work on phonon hydrodynamic model and its thermodynamic derivation relies on the simplified assumption of gray Debye model. It remains a challenging task to consider the more realistic non-linear dispersion and spectral lifetime of phonons in future study.

**Acknowledgments:** The authors also appreciate helpful discussions with Prof. D. Jou and Prof. S.Y. Chen. Y.G. would like to appreciate the financial support of the starting-up funding (AUGA2160500923) from Harbin Institute of Technology and the NSF Fund for Excellent Young Scientists Fund Program (Overseas).

**Research ethics:** Not applicable.

**Author contributions:** The authors have accepted responsibility for the entire content of this manuscript and approved its submission.

**Conflict of interest:** The authors state no conflict of interest.

**Research funding:** This work is financially supported by the starting-up funding from Harbin Institute of Technology, the NSF Fund for Excellent Young Scientists Fund Program (Overseas), the NSF grant of China (No. 12272207) and the National Key R&D Program of China (No. 2019YFA0708704).

**Data availability:** Not applicable.

## References

- [1] C.-M. Ho and Y.-C. Tai, “Micro-electro-mechanical-systems (MEMS) and fluid flows,” *Annu. Rev. Fluid Mech.*, vol. 30, pp. 579–612, 1998.
- [2] G. Karniadakis, A. Beskok, and N. Aluru, *Microflows and Nanoflows: Fundamentals and Simulation*, New York, Springer, 2005.
- [3] A. Alizadeh, W. L. Hsu, M. Wang, and H. Daiguji, “Electroosmotic flow: from microfluidics to nanofluidics,” *Electrophoresis*, vol. 42, no. 7–8, pp. 834–868, 2021.
- [4] M. Beidaghi and Y. Gogotsi, “Capacitive energy storage in micro-scale devices: recent advances in design and fabrication of micro-supercapacitors,” *Energy Environ. Sci.*, vol. 7, no. 3, pp. 867–884, 2014.
- [5] G. He, *et al.*, “Nanostructured ion-exchange membranes for fuel cells: recent advances and perspectives,” *Adv. Mater.*, vol. 27, no. 36, pp. 5280–5295, 2015.
- [6] A. L. Moore and L. Shi, “Emerging challenges and materials for thermal management of electronics,” *Mater. Today*, vol. 17, no. 4, pp. 163–174, 2014.
- [7] Y. Cui, M. Li, and Y. Hu, “Emerging interface materials for electronics thermal management: experiments, modeling, and new opportunities,” *J. Mater. Chem. C*, vol. 8, no. 31, pp. 10568–10586, 2020.
- [8] A. J. Minnich, M. S. Dresselhaus, Z. F. Ren, and G. Chen, “Bulk nanostructured thermoelectric materials: current research and future prospects,” *Energy Environ. Sci.*, vol. 2, no. 5, pp. 466–479, 2009.
- [9] R. R. Gattass and E. Mazur, “Femtosecond laser micromachining in transparent materials,” *Nat. Photonics*, vol. 2, no. 4, pp. 219–225, 2008.
- [10] D. Y. Li, Y. Y. Wu, P. Kim, L. Shi, P. D. Yang, and A. Majumdar, “Thermal conductivity of individual silicon nanowires,” *Appl. Phys. Lett.*, vol. 83, no. 14, pp. 2934–2936, 2003.
- [11] C.-W. Chang, D. Okawa, H. Garcia, A. Majumdar, and A. Zettl, “Breakdown of Fourier’s law in nanotube thermal conductors,” *Phys. Rev. Lett.*, vol. 101, no. 7, p. 075903, 2008.
- [12] N. Yang, G. Zhang, and B. Li, “Violation of Fourier’s law and anomalous heat diffusion in silicon nanowires,” *Nano Today*, vol. 5, no. 2, pp. 85–90, 2010.
- [13] M. Wang, N. Yang, and Z.-Y. Guo, “Non-Fourier heat conductions in nanomaterials,” *J. Appl. Phys.*, vol. 110, no. 6, p. 064310, 2011.
- [14] H. Grad, “On the kinetic theory of rarefied gases,” *Commun. Pure Appl. Math.*, vol. 2, no. 4, pp. 331–407, 1949.
- [15] H. Struchtrup and M. Torrilhon, “Regularization of Grad’s 13 moment equations: derivation and linear analysis,” *Phys. Fluids*, vol. 15, no. 9, pp. 2668–2680, 2003.
- [16] Y. Guo and M. Wang, “Phonon hydrodynamics and its applications in nanoscale heat transport,” *Phys. Rep.*, vol. 595, pp. 1–44, 2015.
- [17] F. X. Alvarez, D. Jou, and A. Sellitto, “Phonon hydrodynamics and phonon-boundary scattering in nanosystems,” *J. Appl. Phys.*, vol. 105, no. 1, p. 014317, 2009.
- [18] Y. Guo and M. Wang, “Phonon hydrodynamics for nanoscale heat transport at ordinary temperatures,” *Phys. Rev. B*, vol. 97, no. 3, p. 035421, 2018.
- [19] L. Onsager, “Reciprocal relations in irreversible thermodynamics I,” *Phys. Rev.*, vol. 37, no. 4, pp. 405–426, 1931.
- [20] I. Prigogine, *Etude thermodynamique des processus irréversibles*, Liege, Paris, Desoer, 1947.

- [21] V. A. Cimmelli, A. Sellitto, and D. Jou, "Nonlocal effects and second sound in a nonequilibrium steady state," *Phys. Rev. B*, vol. 79, no. 1, p. 014303, 2009.
- [22] V. A. Cimmelli, A. Sellitto, and D. Jou, "Nonequilibrium temperatures, heat waves, and nonlinear heat transport equations," *Phys. Rev. B*, vol. 81, no. 5, p. 054301, 2010.
- [23] M. Criado-Sancho and J. Llebot, "Behavior of entropy in hyperbolic heat conduction," *Phys. Rev. E*, vol. 47, no. 6, pp. 4104–4107, 1993.
- [24] I. Müller and T. Ruggeri, *Rational Extended Thermodynamics*, New York, Springer, 1998.
- [25] D. Jou, J. Casas-Vázquez, and G. Lebon, *Extended Irreversible Thermodynamics*, Heidelberg, Springer, 2010.
- [26] H. Struchtrup and M. Torrilhon, "H theorem, regularization, and boundary conditions for linearized 13 moment equations," *Phys. Rev. Lett.*, vol. 99, no. 1, p. 014502, 2007.
- [27] D. Jou and J. Casas-Vázquez, "Nonequilibrium absolute temperature, thermal waves and phonon hydrodynamics," *Physica A*, vol. 163, no. 1, pp. 47–58, 1990.
- [28] A. Valenti, M. Torrisi, and G. Lebon, "Heat pulse propagation by second sound in dielectric crystals," *J. Phys.: Condens. Matter*, vol. 9, no. 15, pp. 3117–3127, 1997.
- [29] M. Wang, J. Liu, and S. Chen, "Electric potential distribution in nanoscale electroosmosis: from molecules to continuum," *Mol. Simul.*, vol. 34, no. 5, pp. 509–514, 2008.
- [30] H. Tian, W. Huang, M. Li, and M. Wang, "Critical size of continuum theory applicability for single-phase liquid flow in nanochannel," *J. Nanosci. Nanotechnol.*, vol. 17, no. 9, pp. 6149–6158, 2017.
- [31] A. Bejan, "A study of entropy generation in fundamental convective heat transfer," *J. Heat Transfer*, vol. 101, no. 4, pp. 718–725, 1979.
- [32] A. Bejan, *Entropy Generation Minimization*, New York, CRC Press, 1996.
- [33] H. Herwig, "The role of entropy generation in momentum and heat transfer," *J. Heat Transfer*, vol. 134, no. 3, p. 031003, 2012.
- [34] M. Avci and O. Aydin, "Second-law analysis of heat and fluid flow in microscale geometries," *Int. J. Exergy*, vol. 4, no. 3, pp. 286–301, 2007.
- [35] K. Hooman, "Entropy generation for microscale forced convection: effects of different thermal boundary conditions, velocity slip, temperature jump viscous dissipation, and duct geometry," *Int. Commun. Heat Mass Transfer*, vol. 34, no. 8, pp. 945–957, 2007.
- [36] M. Yari, "Second-law analysis of flow and heat transfer inside a microannulus," *Int. Commun. Heat Mass Transfer*, vol. 36, no. 1, pp. 78–87, 2009.
- [37] A. Sadeghi and M. H. Saidi, "Second law analysis of slip flow forced convection through a parallel plate microchannel," *Nanoscale Microscale Thermophys. Eng.*, vol. 14, no. 4, pp. 209–228, 2010.
- [38] L. Kuddusi, "First and second law analysis of fully developed gaseous slip flow in trapezoidal silicon microchannels considering viscous dissipation effect," *Int. J. Heat Mass Transfer*, vol. 54, no. 1–3, pp. 52–64, 2011.
- [39] Y. Guo and M. Wang, "Thermodynamic analysis of gas flow and heat transfer in microchannels," *Int. J. Heat Mass Transfer*, vol. 103, pp. 773–782, 2016.
- [40] S. R. De Groot and P. Mazur, *Non-Equilibrium Thermodynamics*, New York, Dover Publications, 1962.
- [41] S. Chapman and T. G. Cowling, *The Mathematical Theory of Non-Uniform Gases*, Cambridge, Cambridge University Press, 1953.
- [42] P. L. Bhatnagar, E. P. Gross, and M. Krook, "A model for collision processes in gases. I. small amplitude in charged and neutral one-component systems," *Phys. Rev.*, vol. 94, no. 3, pp. 511–525, 1954.
- [43] G. M. Kremer, *An Introduction to the Boltzmann Equation and Transport Processes in Gases*, Heidelberg, Springer, 2010.
- [44] O. Aydin and M. Avci, "Heat and fluid flow characteristics of gases in micropipes," *Int. J. Heat Mass Transfer*, vol. 49, no. 9–10, pp. 1723–1730, 2006.
- [45] R. A. Guyer and J. A. Krumhansl, "Solution of the linearized phonon Boltzmann equation," *Phys. Rev.*, vol. 148, no. 2, pp. 766–778, 1966.
- [46] S. Both, B. Czél, T. Fülöp, G. Gróf, Á. Gyenis, R. Kovács, P. Ván, and J. Verhás, "Deviation from the Fourier law in room-temperature heat pulse experiments," *J. Non-Equilib. Thermodyn.*, vol. 41, no. 1, pp. 41–48, 2016.
- [47] P. Ván, A. Berezovski, T. Fülöp, G. Gróf, R. Kovács, Á. Lovas, and J. Verhás, "Guyer-Krumhansl-type heat conduction at room temperature," *Europhys. Lett.*, vol. 118, no. 5, p. 50005, 2017.
- [48] A. Fehér, N. Lukács, L. Somlai, T. Fodor, M. Szücs, T. Fülöp, P. Ván, and R. Kovács, "Size effects and beyond-Fourier heat conduction in room-temperature experiments," *J. Non-Equilib. Thermodyn.*, vol. 46, no. 4, pp. 403–411, 2021.
- [49] W. Dreyer and H. Struchtrup, "Heat pulse experiments revisited," *Contin. Mech. Thermodyn.*, vol. 5, no. 1, pp. 3–50, 1993.
- [50] Y. Guo, D. Jou, and M. Wang, "Nonequilibrium thermodynamics of phonon hydrodynamic model for nanoscale heat transport," *Phys. Rev. B*, vol. 98, no. 10, p. 104304, 2018.
- [51] V. A. Cimmelli, "Different thermodynamic theories and different heat conduction laws," *J. Non-Equilib. Thermodyn.*, vol. 34, no. 4, pp. 299–333, 2009.
- [52] G. Lebon, "Heat conduction at micro and nanoscales: a review through the prism of Extended Irreversible Thermodynamics," *J. Non-Equilib. Thermodyn.*, vol. 39, no. 1, pp. 35–59, 2014.
- [53] D. Jou, G. Lebon, and M. Criado-Sancho, "Variational principles for thermal transport in nanosystems with heat slip flow," *Phys. Rev. E*, vol. 82, no. 3, p. 031128, 2010.

- [54] G. Lebon, D. Jou, and P. C. Dauby, “Beyond the Fourier heat conduction law and the thermal no-slip boundary condition,” *Phys. Lett. A*, vol. 376, no. 45, pp. 2842–2846, 2012.
- [55] J. E. Turney, A. J. H. McGaughey, and C. H. Amon, “In-plane phonon transport in thin films,” *J. Appl. Phys.*, vol. 107, no. 2, p. 024317, 2010.
- [56] R. A. Guyer and J. A. Krumhansl, “Thermal conductivity, second sound, and phonon hydrodynamic phenomena in nonmetallic crystals,” *Phys. Rev.*, vol. 148, no. 2, pp. 778–788, 1966.
- [57] L. Sendra, A. Beardo, P. Torres, J. Bafaluy, F. X. Alvarez, and J. Camacho, “Derivation of a hydrodynamic heat equation from the phonon Boltzmann equation for general semiconductors,” *Phys. Rev. B*, vol. 103, no. 14, p. L140301, 2021.